



## Solid state investigation and characterization of the polymorphic and pseudopolymorphic forms of indapamide

Pradeep Ghugare<sup>a,b,c,\*</sup>, Vaijanath Dongre<sup>c</sup>, Pravin Karmuse<sup>b,c</sup>, Ragnesh Rana<sup>b</sup>, Dharmendra Singh<sup>b</sup>, Ashok Kumar<sup>b</sup>, Zoeb Filmwala<sup>a</sup>

<sup>a</sup> Nadkarni Sacasa Research Laboratory, Department of Chemistry, St. Xavier's College, Mumbai 400001, India

<sup>b</sup> Ipca Laboratories Ltd., Chemical Research Division, Kandivli Industrial Estate, Kandivli (W), Mumbai 400 067, India

<sup>c</sup> Department of Chemistry, University of Mumbai, Vidyayagari, Kalina, Santacruz (E), Mumbai 400 098, India

### ARTICLE INFO

#### Article history:

Received 15 January 2009

Received in revised form 31 August 2009

Accepted 5 September 2009

Available online 11 September 2009

#### Keywords:

Indapamide

Polymorphs

Pseudopolymorphs

XRPD

Solid state characterization

### ABSTRACT

Solid state investigation and polymorphic screening of indapamide, a diuretic drug generally used for the treatment of hypertension was carried out. Substantial differences were obtained in the solid state properties of crystals confirming the existence of a polymorphic and three pseudopolymorphic forms of indapamide. Detailed methods of preparation of the polymorphs and pseudopolymorphs are described. X-ray powder diffraction (XRPD), diffuse reflectance infrared Fourier transform (DRIFT) spectroscopy, differential scanning calorimetry (DSC) and thermogravimetric analysis (TGA) were employed for the characterization of different crystalline forms of indapamide. The stoichiometric ratio of solvents associated with the drug molecules in the pseudopolymorphic forms were calculated using TGA, nuclear magnetic resonance (NMR) spectroscopy and headspace gas chromatographic (HS-GC) analysis.

© 2009 Elsevier B.V. All rights reserved.

## 1. Introduction

Indapamide (Fig. 1), a non-thiazide sulfonamide diuretic drug is primarily used in the treatment of hypertension as well as edema caused by congestive heart failure. It works by preventing the kidney from reabsorbing salt and water that is destined to be eliminated in the urine. The loss of salt from the muscle causes the muscle to relax and the relaxation of the vessels result in reduced blood pressure [1–3].

Polymorphism is defined as the ability of a substance to exist as two or more crystalline phases or forms that have different arrangements and/or conformations of the molecule in crystal lattice [4]. Crystalline polymorphs have same chemical composition but different crystal structures. Solvates, also known as pseudopolymorphs are crystalline solid adducts containing solvent molecules in the crystal structure, in stoichiometric or non-stoichiometric proportions, giving rise to unique difference in the physical and chemical properties of drug. The pharmaceutical solids having

different chemical and physical properties can affect the bioavailability and stability of the drug [5–7]. The various effects of pharmaceutical processing on the drug polymorphs, solvates and phase transitions are described in detail by Brittain and Fiese [8]. Identification and characterization of polymorphic behavior in a pharmaceutical substance is therefore, an essential aspect of drug development.

The possibility of polymorphism or pseudopolymorphism may exist for any particular compound, but the conditions required for unknown polymorphs or pseudopolymorphs are not easily determined [9]. It has been estimated that large number of pharmaceuticals exhibit polymorphism. For example, 70% of barbiturates, 60% of sulfonamides and 23% of steroids are believed to exist in different polymorphic and pseudopolymorphic forms [10]. Number of reports describing the polymorphic behavior of sulfonamides is available in the literature [11–15].

Crystal structure of commercial form of indapamide using powder diffraction data has been reported, [16] wherein the authors demonstrated the presence of 3% water in commercial indapamide, [17] due to its existence as a non-stoichiometric hydrate form. To date, however, no reports are available on the polymorphic and pseudopolymorphic forms of indapamide in the literature. Present work describes the investigation and characterization of a new polymorphic and three pseudopolymorphic forms (solvates) using DSC, TGA, XRPD and DRIFT techniques.

\* Corresponding author at: Nadkarni Sacasa Research Laboratory, Department of Chemistry, St. Xavier's College, Mumbai 400001, India. Tel.: +91 22 66474756.

E-mail addresses: [p.d.ghugare@yahoo.com](mailto:p.d.ghugare@yahoo.com) (P. Ghugare), [dr.zoab@yahoo.com](mailto:dr.zoab@yahoo.com) (Z. Filmwala).

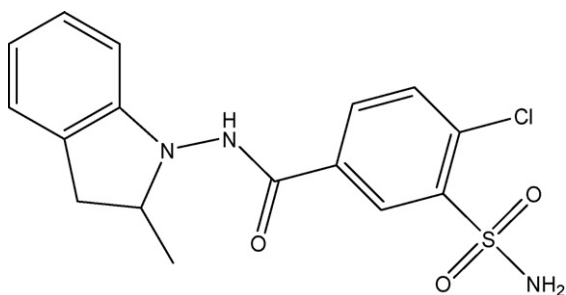


Fig. 1. Chemical structure of indapamide.

## 2. Experimental

### 2.1. Materials and reagents

The indapamide bulk drug sample was obtained from Chemical Research Division, Ipca laboratories Ltd., Mumbai, India. Laboratory grade solvents used for crystallization, analytical grade solvents used for HS-GC and KBr used for DRIFT analysis were purchased from Merck KGaA, Darmstadt, Germany. Analytical grade *N,O*-bis-(trimethylsilyl) trifluoro acetamide (BSTFA) was purchased from Spectrochem, Mumbai, India. Dimethyl sulfoxide- $d_6$  and tetramethylsilane for NMR were from Aldrich Chemical Co. Milwaukee, WI, USA. Hydranal Composite5 used for Karl fisher titrimetry was purchased from Riedel de Haen, Seelze, Germany.

### 2.2. Methods

Indapamide is soluble in acetonitrile, ethyl acetate, glacial acetic acid, methanol, ethanol and other alcoholic solvents. It is very slightly soluble in ether and chloroform, while practically insoluble in water. Various crystallization experiments were carried out using individual as well as combinations of solvents at normal and elevated temperature. Polymorphic screening of samples using XRPD and TGA was carried out to check formation of polymorphic and pseudopolymorphic forms.

#### 2.2.1. Preparation of anhydrous form (form-I)

A saturated suspension of indapamide prepared by adding excess of indapamide in glacial acetic acid was maintained at 65–70 °C with constant stirring for 2 h. Small portion of the mixture was removed after regular time interval of 30 min and dried. The melting point of the dried compound was measured. Initially, melting point of the compound was in the range of 168–175 °C. After 2 h, the melting temperature shifted to the range of 185–193 °C, heating was then stopped and the suspension was allowed to cool to room temperature. The solid obtained was separated from the solution by vacuum filtration and dried at 50–55 °C for 2–3 h under vacuum.

#### 2.2.2. Preparation of solvates

The saturated solutions of indapamide in acetone were prepared in three different 250 ml flasks and maintained at 35 °C with constant stirring. In order to prepare different solvates equal volume of carbon tetrachloride, cyclohexane and diethyl ether were slowly added to the respective flask. After complete addition, the solutions were kept at 35 °C for about half an hour and then cooled to room temperature. The precipitates formed were filtered by vacuum filtration followed by washing with excess amount of respective precipitating solvent. The solids obtained were dried at 50–55 °C under vacuum. Formation of solvates was checked by TGA analysis. The samples precipitated using carbon tetrachloride, cyclohexane and diethyl ether were labeled as solvate-I, solvate-II and solvate-III, respectively.

### 2.3. Stability studies

In order to test ability to uptake water, samples of form-I, solvate-I, II and III were stored at room temperature in open air (about 55% RH) and in a desiccator for 1 year. Samples including the commercial form were also subjected for manual grinding using mortar and pestle to study physical stability and solid–solid transition. The resulting samples were analyzed for solid state transition by DRIFT, water content by TGA and Karl Fischer titrimetry (KFT).

### 2.4. Instrumentation

#### 2.4.1. Scanning electron microscopy (SEM)

The SEM images were obtained on a JSM-6360A system (JEOL, Tokyo, Japan), using an acceleration potential of 10 kV. The samples were sputter coated with platinum to eliminate charging effects.

#### 2.4.2. Diffuse reflectance infrared Fourier transform (DRIFT) spectroscopy

The DRIFT spectra were recorded in the solid state as KBr powder dispersion using a Spectrum One FT-IR spectrometer (PerkinElmer, Beaconsfield, UK) equipped with diffuse reflectance sampling accessory. The spectrum for each sample was recorded with an average of 16 co-added scans in transmission mode over a spectral region of 450–4000  $\text{cm}^{-1}$  with a resolution of 4  $\text{cm}^{-1}$ .

#### 2.4.3. X-ray powder diffraction (XRPD)

XRPD patterns of samples were recorded at room temperature on an X'Pert PRO diffractometer (PANalytical, Almelo, The Netherlands) with Cu K $\alpha$  radiation, ( $\lambda = 1.5406 \text{ \AA}$ ) passing through nickel filter, divergence slit (10 mm), antiscattering slit (10 mm) and soller slit (0.02 rad). The X-ray generator was set at a voltage of 45 kV and current of 40 mA. The diffractometer was calibrated for accuracy of peak positions with silicon powder (ASTM-692). Samples were subjected to XRPD analysis in continuous mode with a step size of 0.008°  $2\theta$  and step time of 15 s over an angular range of 3–40°  $2\theta$ . To minimize the preferred orientations, the samples were prepared by back loading technique using the PW1770/10 sample preparation kit. The sample holder was rotated in a plane parallel to its surface at the speed of 30 rpm during the measurements. Obtained diffractograms were analyzed with X'Pert HighScore Plus diffraction software (version 2.1b).

#### 2.4.4. Thermal analysis (DSC and TGA)

DSC thermograms were recorded on a Q-100 instrument (TA Instruments, New Castle, DE, USA). Samples weighing 2–3 mg were heated in crimped aluminum pans with pierced lead from 30 to 210 °C at the rate of 10 °C/min. Nitrogen was used as a purging gas under ambient flow rate.

The mass loss of the sample as a function of temperature was determined using a TGA Q-500 instrument (TA Instruments, New Castle, DE, USA). The samples were placed in open platinum crucibles and heated at the rate of 25 °C/min in the range of 30–400 °C under a nitrogen purge (20 ml/min). The DSC and TGA data was processed using Universal Analysis 2000 software (version 4.3A).

#### 2.4.5. Nuclear magnetic resonance (solution-state)

NMR spectra were obtained on a 400 MHz instrument (Bruker, Faellanden, Switzerland). The spectra were processed with XWIN NMR software (version 3.1). The samples were prepared by dissolving 5 mg of each form in 600  $\mu\text{l}$  of DMSO- $d_6$  spiked with 0.03% of tetramethylsilane as reference ( $\delta H = 0 \text{ ppm}$ ).

#### 2.4.6. Headspace gas chromatography (HS-GC)

A 6890 series gas chromatographic system (Agilent, Wilmington, DE, USA) equipped with flame ionization detector and Gerstel

MPS2 headspace was used for HS-GC analysis. Chromatographic data were collected and processed using ChemStation software.

An Rtx-624 (30.0 mm × 0.53 mm i.d.; 3.0 μ) capillary column (Restek, Bellefonte, PA, USA) was used for chromatographic determination of acetic acid and DB-5 (30.0 mm × 0.53 mm i.d.; 5.0 μ) capillary column (J & W Scientific, Folsom, CA, USA) was used for the determination of other solvents. Nitrogen was used as a carrier gas at a flow rate of 2.0 ml/min. Injection was carried out in split mode, with a split ratio of 50:1. The injector and detector temperature were set at 200 and 240 °C, respectively. The oven temperature was initially set at 50 °C for 10 min, and then it was raised by 10 °C/min to 220 °C and left constant for 10 min. The headspace oven temperature was set at 90 °C with thermostating time 20 min. The needle temperature was 100 °C. Pressurization time was 3.0 min and the injection volume was 0.5 ml. Vial pressure was set at 15 psi and the headspace carrier was regulated at 25 ml/min. Standard solutions of solvents (5000 ppm) and sample solutions of anhydrous and solvate form (50,000 ppm) were prepared in dimethylformamide. For acetic acid determination 10% of *N,O*-bis-(trimethylsilyl) trifluoro acetamide was added to the standard and sample solution.

#### 2.4.7. Karl Fischer titrimetry (KFT)

The water content of the samples was determined with a DL-18 (Mettler, Schwerzenbach, Switzerland) titrator apparatus. Samples (80–90 mg) were quickly transferred to the titration vessel containing anhydrous dimethylformamide and titrated using Hydranal Composite5.

### 3. Results and discussion

#### 3.1. Polymorphic screening

To investigate the solid state behavior of indapamide, samples recrystallized from various solvent systems were screened using XRPD and TGA. The screening revealed the formation of an anhydrous polymorph (form-I) and three solvate forms of indapamide. Commercial hydrate form of indapamide was reobtained from the solutions prepared in isopropyl alcohol, acetic acid and ethanol after precipitation with water. The form-I was obtained by recrystallizing indapamide from acetic acid at 65–70 °C. Solvate-I, II and III were obtained by recrystallizing indapamide at 35 °C, from mixtures of acetone: carbon tetrachloride, acetone: cyclo-

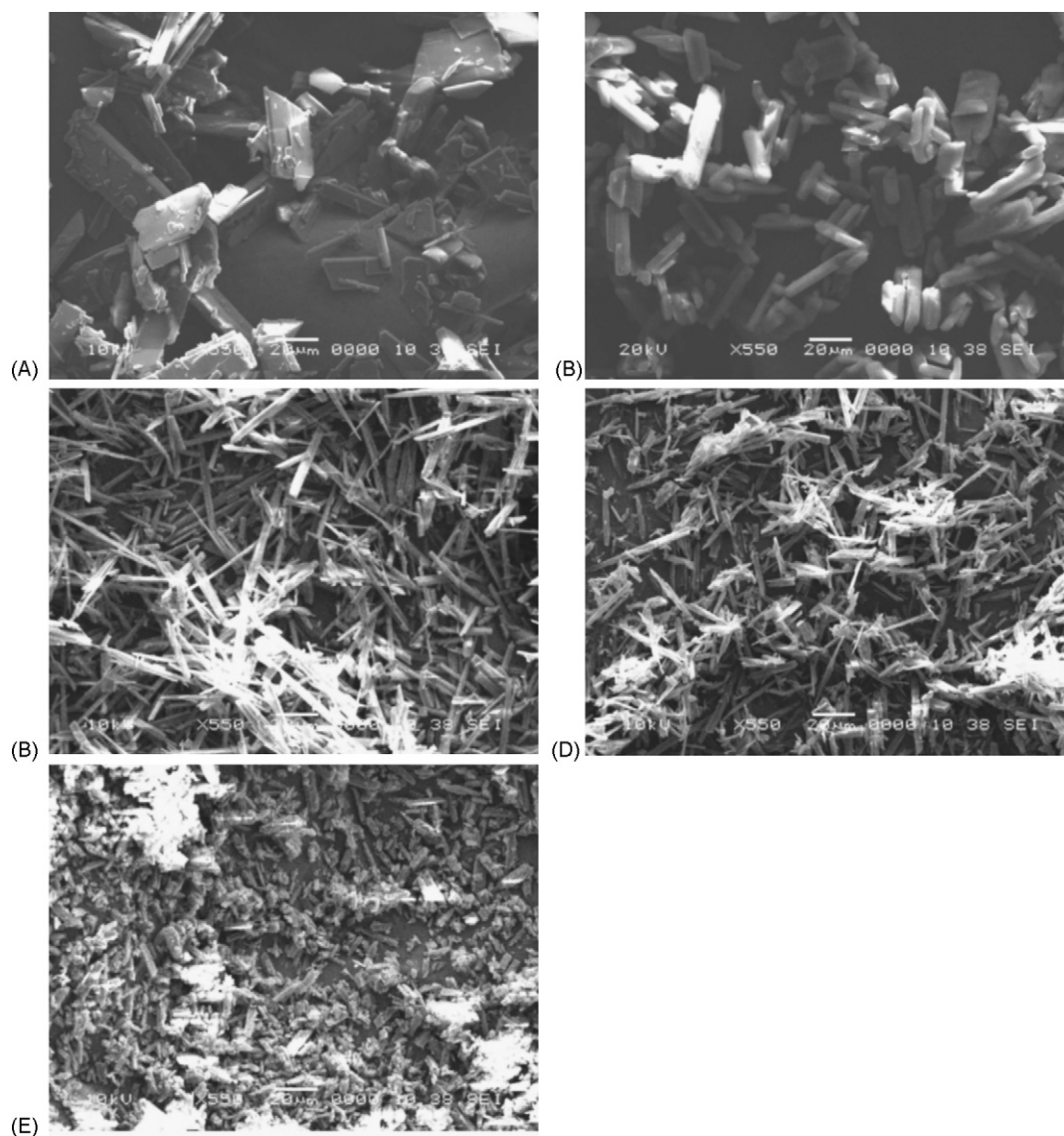


Fig. 2. SEM images highlighting the different morphologies of (A) commercial form, (B) form-I, (C) solvate-I, (D) solvate-II and (E) solvate-III.

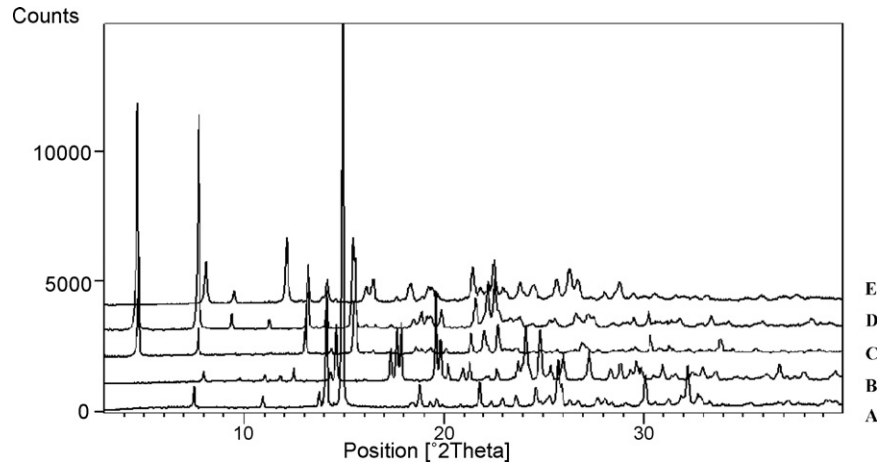


Fig. 3. Comparison of XRPD patterns of indapamide: (A) commercial form, (B) form-I, (C) solvate-I, (D) solvate-II and (E) solvate-III.

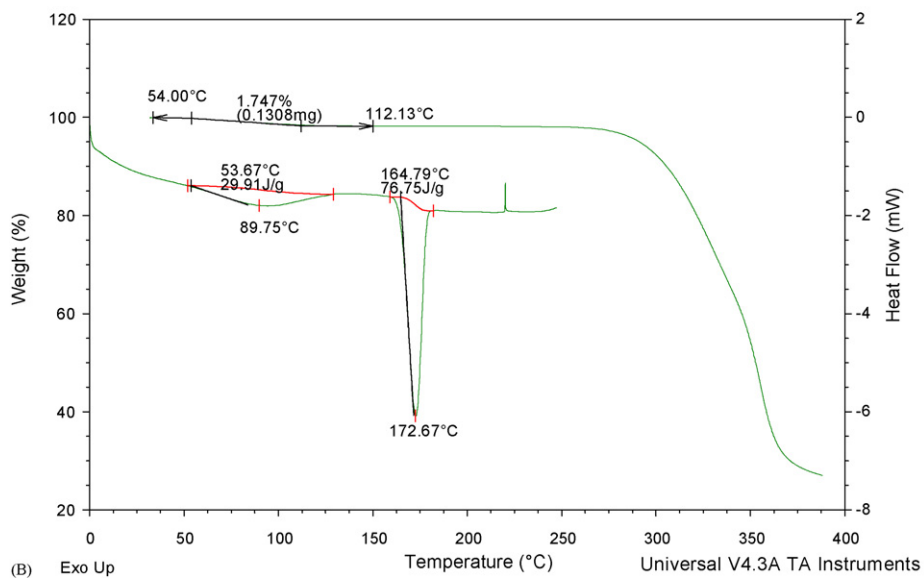
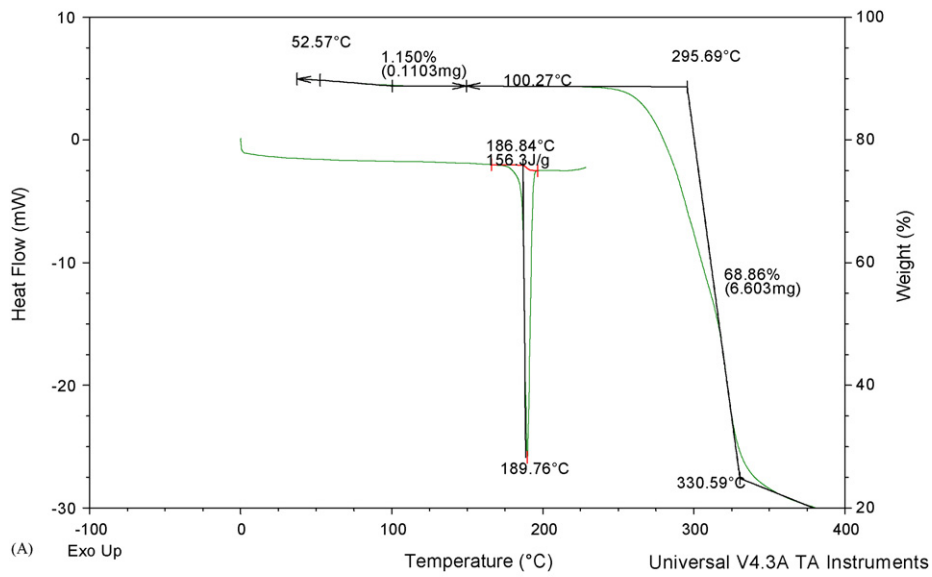
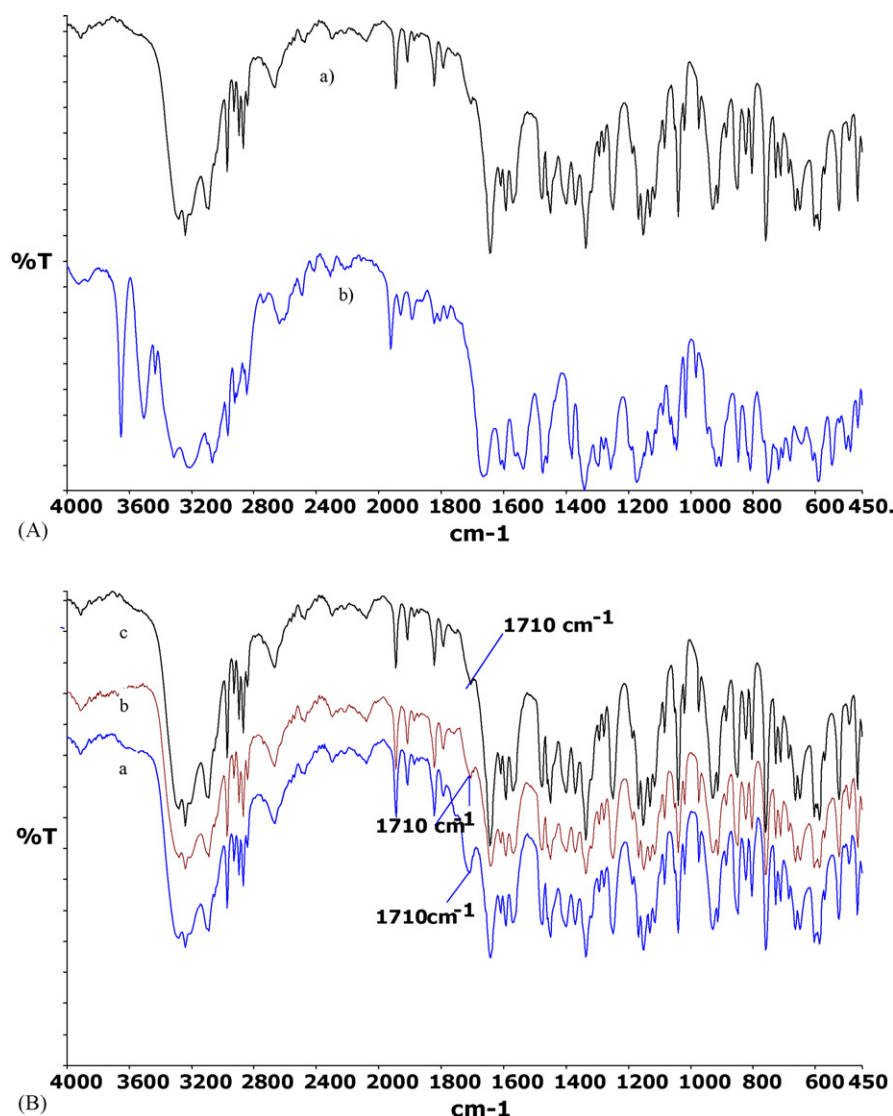


Fig. 4. Comparison of thermograms (DSC and TGA) of indapamide: (A) form-I and (B) commercial form.



**Fig. 5.** (A) FTIR spectra of indapamide: (a) form-I and (b) commercial hydrate. (B) FTIR spectra of indapamide form-I by subsequent washings with water (a–c) showing elimination of peak at  $1710\text{ cm}^{-1}$  (carbonyl stretching of acetic acid).

hexane and acetone: diethyl ether, respectively. The solvates were also obtained by recrystallization process in which acetone is replaced by other solvents like ethyl acetate or acetic acid. The water content of the commercial form samples was found to be in the range of 2.5–3.5%. Polymorphic characterization data of solvate-I, II, III and form-I were compared with that of commercial form.

### 3.2. Characterization of anhydrous form (form-I)

The morphological analysis using SEM showed flat plate like structure for commercial form and cylindrical tube like structure for form-I (Fig. 2). The X-ray powder diffractograms of both forms showed distinct differences in peak positions and relative intensities (Fig. 3). The form-I showed characteristic peaks at  $7.98^\circ$ ,  $10.99^\circ$ ,  $11.80^\circ$ ,  $17.34^\circ$ ,  $17.68^\circ$  and  $17.90^\circ$   $2\theta$  those corresponding only to the form-I, while the commercial form showed characteristic peaks at  $7.50^\circ$ ,  $13.77^\circ$ ,  $14.13^\circ$ ,  $18.77^\circ$  and  $21.81^\circ$   $2\theta$ . The water content for the form-I was 0.11%. The comparison of XRPD patterns of form-I and commercial form showed that they exhibit different arrangement of molecules in the crystal lattice.

DSC thermogram of form-I showed an endothermic peak with maxima at  $189^\circ\text{C}$  (enthalpy of fusion,  $\Delta H_f = 156.3\text{ J/g}$ ) due to melting (Fig. 4). TGA analysis revealed no loss from the sample over temperature range of  $30\text{--}250^\circ\text{C}$ . DSC thermogram of commercial form showed a broad endothermic peak over the range of  $53.6\text{--}112^\circ\text{C}$  due to water loss followed by a sharp endothermic peak with maxima at  $172.67^\circ\text{C}$  due to melting ( $\Delta H_f = 76.75\text{ J/g}$ ). The TGA weight loss of the commercial form sample started at room temperature because of the weak hydrogen bond interaction of water molecules in the crystal structure [16].

DRIFT spectra of both the samples were distinctly different (Fig. 5A). The two sharp absorption bands at  $3507$  and  $3654\text{ cm}^{-1}$  for hydroxy functional group of water observed in commercial form were absent in the spectrum of form-I, whereas large variations were seen in the lower frequency region ranging from  $450$  to  $2000\text{ cm}^{-1}$ . A small absorption band observed at  $1710\text{ cm}^{-1}$  for carbonyl stretch in the spectra of form-I was because of traces of free acetic acid in the sample. The sample after repeated washing with water was subjected for DRIFT, wherein the band at  $1710\text{ cm}^{-1}$  was found to be reduced considerably (Fig. 5B). Based on above data form-I was proposed to be a new polymorphic form (form-I) of indapamide.

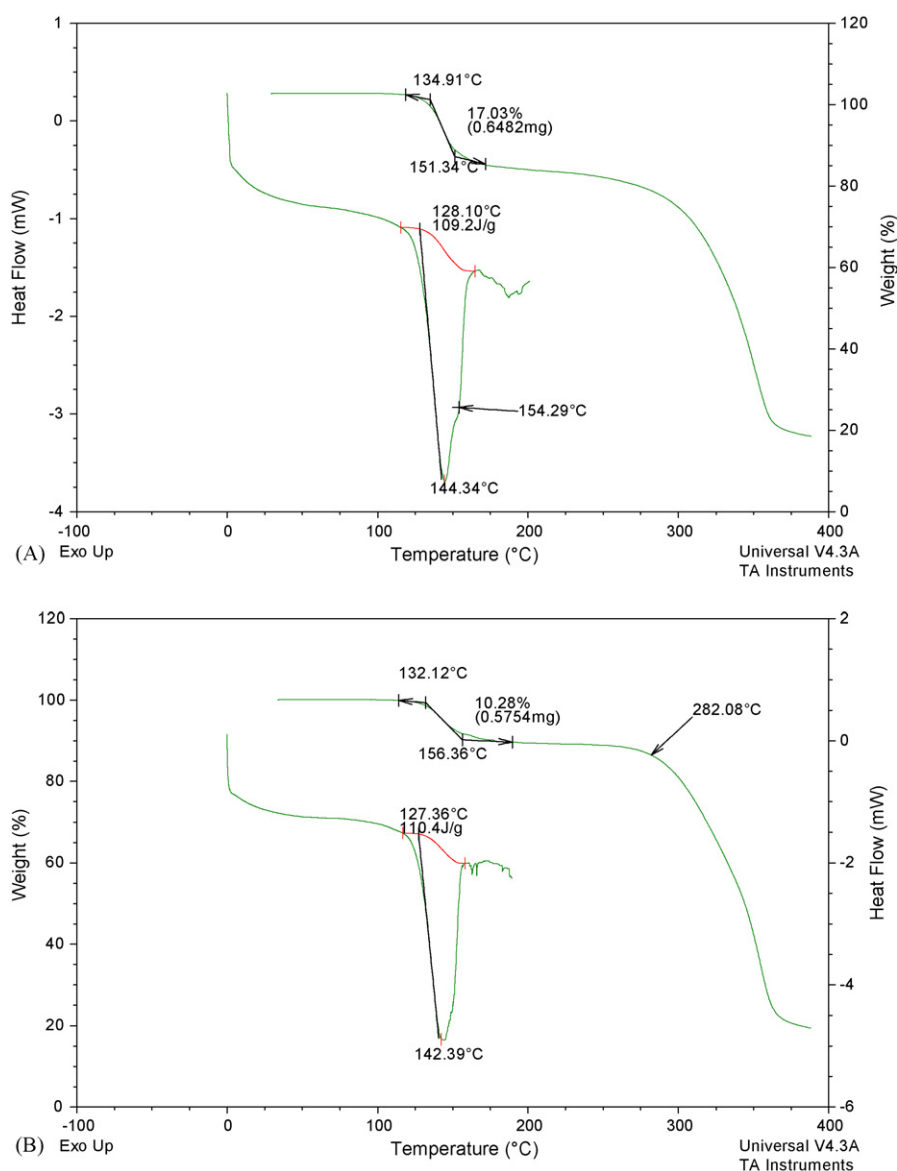


Fig. 6. Comparison of thermograms (DSC and TGA) of indapamide: (A) solvate-I and (B) solvate-II.

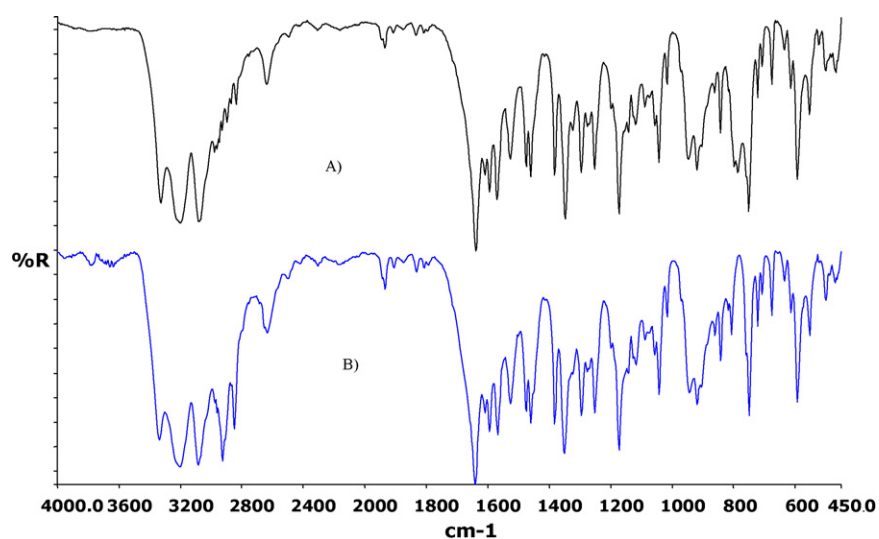


Fig. 7. FTIR spectra of indapamide: (A) solvate-I and (B) solvate-II.



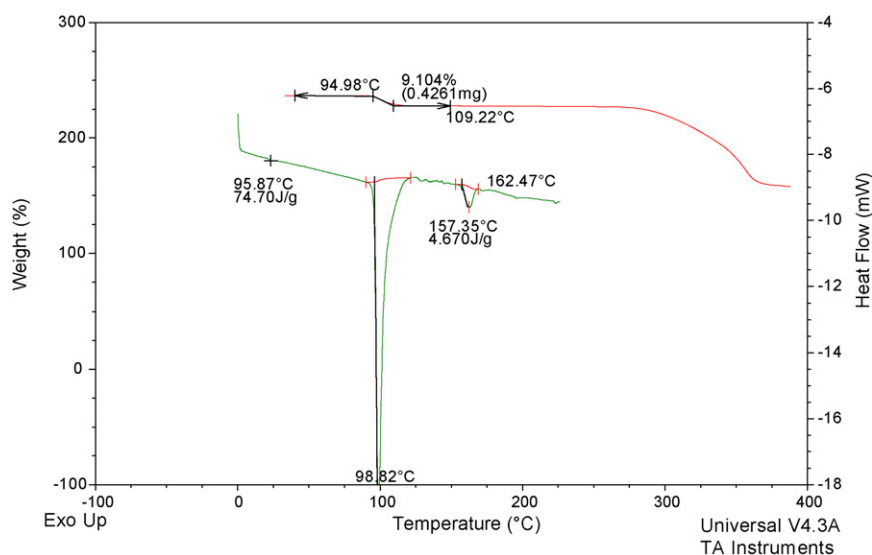


Fig. 8. Comparison of thermograms (DSC and TGA) of indapamide: solvate-III.

### 3.3. Characterization of solvates

The SEM images showed thin lath shaped crystal geometries for solvate-I and II, while fractured lath shaped crystals for solvate-III (Fig. 2). The solvate-I and solvate-II are particularly interesting due to the fact that their SEM, XRPD, DRIFT and DSC profiles largely resembled. The XRPD of both pseudopolymorphs showed similarity in peak positions over  $3\text{--}19^\circ 2\theta$  and  $25\text{--}40^\circ 2\theta$  regions (Fig. 3). DSC thermograms of these solvates showed only a single broad endothermic peak with slight variation in onset temperatures and melting ranges. The onset temperatures for solvate-I and solvate-II were at  $142.33$  and  $144.34^\circ\text{C}$ , while melting ranges were  $132\text{--}153$  and  $129\text{--}156^\circ\text{C}$ , respectively. DSC profiles of the solvates are depicted in Fig. 6. The fundamental frequency positions in the DRIFT spectra of both the solvates were nearly same except slight variations in the range of  $2850\text{--}2950$  and  $780\text{--}788\text{ cm}^{-1}$  (Fig. 7).

TGA analysis, however, was able to clearly differentiate between two solvates. The TGA plot exhibited weight loss of  $18.79\%$  and  $10.62\%$  over the range  $132\text{--}153$  and  $129\text{--}156^\circ\text{C}$  while total weight

loss (decomposition) over  $279\text{--}370$  and  $282\text{--}375^\circ\text{C}$  for solvate-I and solvate-II, respectively (Fig. 6). Based on above observations, the solvates were proposed to be different pseudopolymorphs having isomorphous structure. The similarity in XRPD patterns of drug pseudopolymorphs having isomorphous nature of crystals has been reported in the literature [18].

The XRPD pattern of solvate-III was significantly different as compare to the patterns of other forms and solvates (Fig. 3). It showed characteristic peaks at  $12.13^\circ$ ,  $13.24^\circ$ ,  $14.06^\circ$ ,  $16.40^\circ$ ,  $18.28^\circ$ ,  $19.28^\circ$ ,  $21.43^\circ$ ,  $22.57^\circ$ ,  $26.38^\circ$  and  $26.69^\circ 2\theta$  as compared to the that of form-I. In the DSC thermogram, an endothermic peak was observed with a maxima at  $98.82^\circ\text{C}$  due to the solvent loss followed by melting at  $157.35^\circ\text{C}$  ( $\Delta H_f = 4.67\text{ J/g}$ ) (Fig. 8). TGA plot demonstrated the weight loss of  $9.03\%$  over  $94.98\text{--}109.22^\circ\text{C}$ .

The comparison of DRIFT spectra of solvate-III and commercial form is shown in Fig. 9. Variations were observed in the range  $1300\text{--}1250$ ,  $950\text{--}1000$ ,  $800\text{--}900$  and  $450\text{--}600\text{ cm}^{-1}$  of fingerprint region of the spectra. Two absorption bands at  $3507$  and  $3654\text{ cm}^{-1}$  for hydroxyl group of water observed in the DRIFT spectra of commercial form were absent in the spectra of solvate-III.

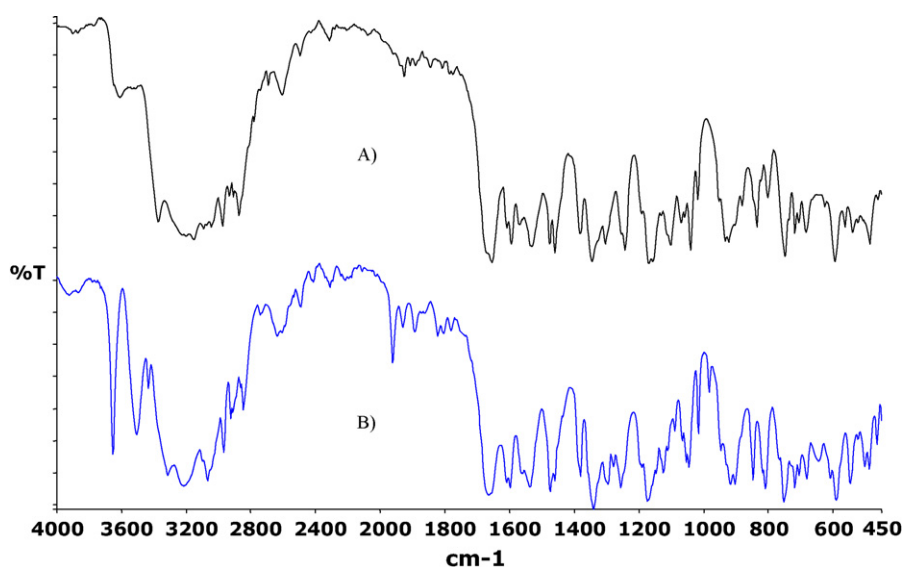


Fig. 9. FTIR spectra of indapamide: (A) solvate-III and (B) commercial form.

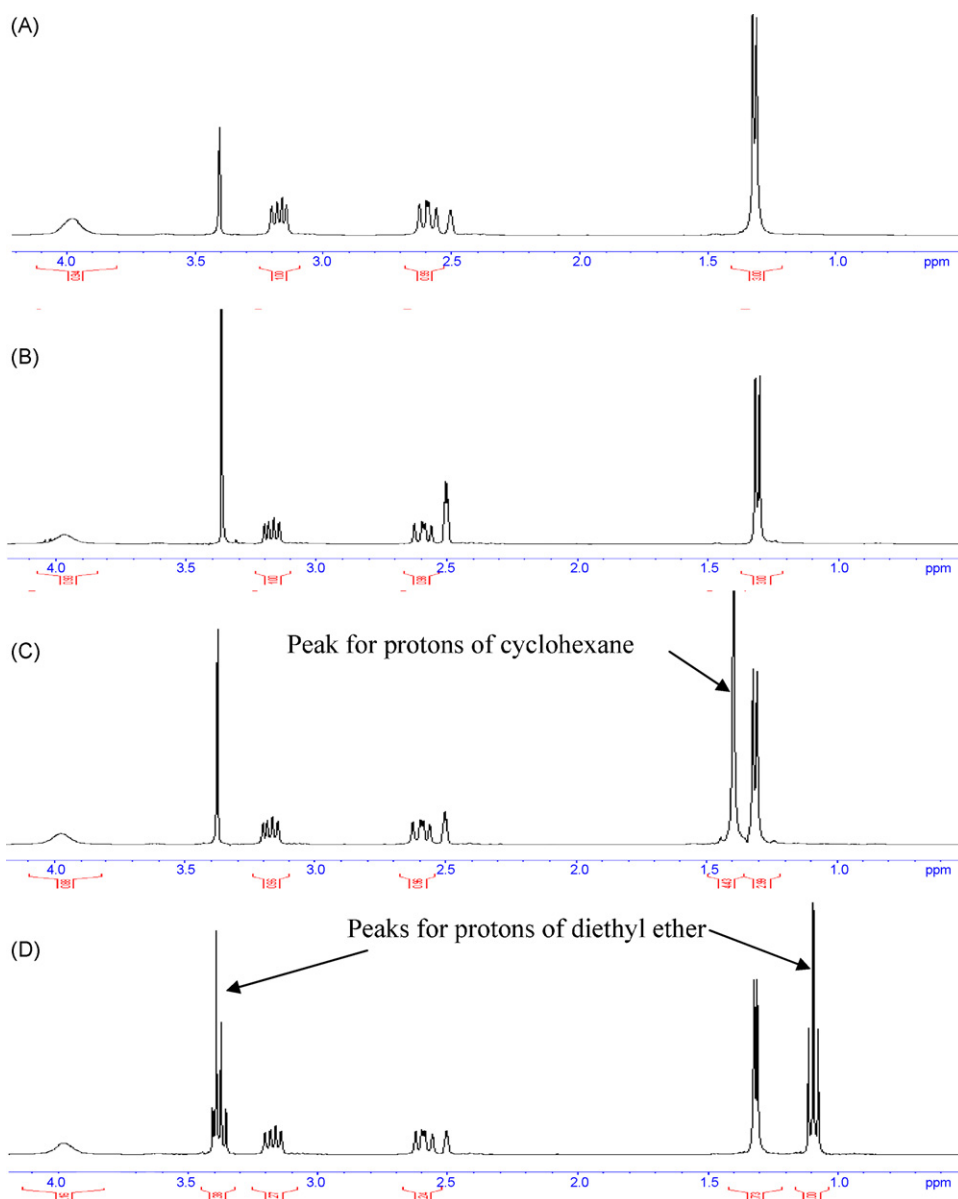


Fig. 10.  $^1\text{H}$  NMR of indapamide (liquid state): (A) form-I, (B) solvate-I, (C) solvate-II and (D) solvate-III.

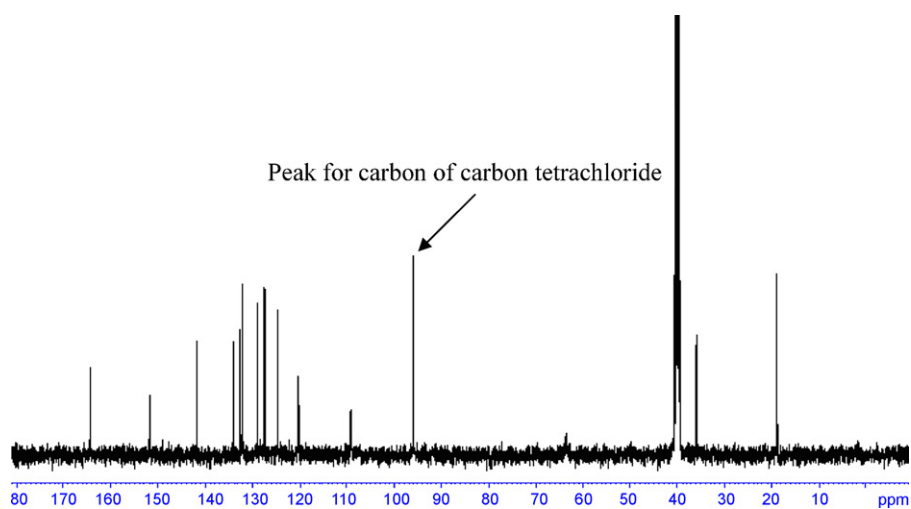


Fig. 11.  $^{13}\text{C}$  NMR of indapamide (liquid state): solvate-I.



**Table 1**

Confirmation of stoichiometry of solvates (A) theoretical weight percentage of the solvents and (B) observed weight loss of solvates in TGA.

Solvents of crystallization	Theoretical weight % (w/w)		
	Mole ratio (indapamide: solvent)		
	1:1	2:1	1:2
(A)			
Cyclohexane	18.71	10.32 <sup>a</sup>	31.46
Diethyl ether	16.85	9.20 <sup>a</sup>	28.70
Carbon tetrachloride	29.48	17.23 <sup>a</sup>	45.62
Acetone	13.71	7.36	24.07
Pseudo polymorphs	Observed weight loss in TGA (w/w)		
(B)			
Solvate-I	17.03		
Solvate-II	10.28		
Solvate-III	9.10		

<sup>a</sup> Calculated weight loss values matching with the observed values.

**Table 2**

HS-GC results of different forms of indapamide.

Sample name	Carbon tetrachloride (%)	Cyclohexane (%)	Diethyl ether (%)	Acetic acid (%)
Form-I	–	–	–	0.21%
Solvate-I	18.11	–	–	–
Solvate-II	–	10.51	–	–
Solvate-III	–	–	9.98	–

### 3.4. Solvent of crystallization and stoichiometry

The calculated weight percentage of solvent by considering either of the solvents used for preparation, were shown in Table 1 with various possible stoichiometric ratios. The comparison of these values with observed weight loss in TGA revealed that the crystals of indapamide in solvate-I, II and III were associated with carbon tetrachloride, cyclohexane and diethyl ether, respectively in 2:1 proportion.

To confirm the identity and proportions of solvent of crystallization, all the solvates were subjected for <sup>1</sup>H NMR analysis. The <sup>1</sup>H NMR of form-I and solvate-I of indapamide showed total signals for ten protons of indapamide (Fig. 10). However, <sup>1</sup>H NMR of solvate-II showed an extra singlet slightly merged with the –CH<sub>3</sub> protons of indapamide at δ 1.31 ppm integrating six protons. This signal confirmed association of half mole of cyclohexane in solvate-II crystals. Similarly <sup>1</sup>H NMR of solvate-III showed an extra triplet integrating two proton at δ 1.06 ppm and an extra quartet integrating three proton at δ 3.36 ppm. These signals can be accounted for half mole of diethyl ether present in the solvate crystals. <sup>13</sup>C NMR of solvate-I showed a signal for carbon at δ 95.9 ppm which confirmed the presence of carbon tetrachloride in the sample (Fig. 11). The peak positions of solvents in <sup>1</sup>H NMR and <sup>13</sup>C NMR was confirmed by independent experiments of individual solvents.

Stoichiometry is further confirmed with the use of HS-GC analysis. The results are shown in Table 2. The standard samples of solvents injected for retention time confirmation showed that carbon tetrachloride and cyclohexane are eluting at same retention time at 17.20 min. Both the solvates showed a major peak for sol-

vents at same retention time. Based on the knowledge of solvents used for the preparation of solvates, it was easily concluded that the solvents associated with solvate-I and II were carbon tetrachloride and cyclohexane, respectively. Also the identities of solvents associated with the solvates were already confirmed by NMR analysis.

### 4. Physical stability and water content variation

The stability and water content variation of samples were investigated at various experimental conditions as described in Section 2.3. All forms were found to be stable and did not show any solid state transition under the experimental conditions. The water content variations were also not significant in all but for the commercial form samples. The water content variation and hydration dehydration studies of commercial form were elaborately described by Smrkoj and Meden [16].

### 5. Conclusion

Based on crystallization experiments and solid state characterization it was concluded that besides the commercial hydrate form, indapamide also exhibit an anhydrous and three solvate forms. The solvates showed stoichiometric ratio of 2:1 with the solvents like diethyl ether, carbon tetrachloride and cyclohexane. Of particular interest, the carbon tetrachloride and cyclohexane solvates were characterized which are having same diffraction properties but different solvent of crystallization.

### Acknowledgements

The authors thank the management of Ipca Laboratories for providing necessary facilities and to Mr. Ganesh Mahale, Mr. Nikhilesh Arya, Mr. Brijesh Sharma and Mr. Sanket Ingle for providing technical assistance. One of the authors Mr. P. D. G. is grateful to Dr. Sanjay M. Nandavadekar for constant encouragement.

### References

- [1] J.G. Hardman, L.E. Limbird, A.G. Gilman, *The Pharmacological Basis of Therapeutics*, tenth ed., McGraw Hill, New York, 2001, pp. 773–774.
- [2] D.A. Abraham, *Burger's Medicinal Chemistry and Drug Discovery*, vol. 3, sixth ed., Wiley, New York, 2003, pp. 83–84.
- [3] J.B. Taylor, D.J. Triggle, *Comprehensive Medicinal Chemistry-II*, vol. 6, Elsevier, UK, 2007, pp. 708–709.
- [4] H. Britain, *Physical Characterization of Pharmaceutical Solids*, Marcel Dekker, New York, 1995.
- [5] J.K. Haleblan, W. Mc Crone, *J. Pharm. Sci.* 58 (1969) 911–929.
- [6] S.R. Bryn, *Solid State Chemistry of Drugs*, second ed., SSCI Inc., Indiana, 1999.
- [7] S.R. Vippagunta, H.G. Brittain, D.J.W. Grant, *Adv. Drug Deliv. Rev.* 48 (2001) 3–26.
- [8] H.G. Brittain, *Polymorphism in Pharmaceutical Solids*, vol. 95, Marcel Dekker, New York, 1999, pp. 331–361.
- [9] Bernstein, *Am. Crystallographic Assoc. Trans.* 39 (2004) 14–23.
- [10] J.K. Haleblan, *J. Pharm. Sci.* 64 (1975) 1269–1288.
- [11] S.S. Yang, J.K. Guillory, *J. Pharm. Sci.* 61 (1972) 26–40.
- [12] C. Baraldia, M.C. Gamberinia, A. Tintin, F. Palazzolia, V. Feriolia, *J. Mol. Struct.* 918 (2009) 88–96.
- [13] R.K.R. Jetti, R. Boese, J.A.R.P. Sarma, L.S. Reddy, P. Vishweshwar, G.R. Desiraju, *Angewandte Chemie* 42 (2003) 1963–1967.
- [14] M.F. Haddow, T. Gelbrich, U.J. Griesser, *Acta Cryst.* C64 (2008) o309–o312.
- [15] U.H. Patel, B.H. Patel, B.N. Patel, *Cryst. Res. Technol.* 36 (2001) 1445–1450.
- [16] M. Smrkoj, A. Meden, *Pharmazie* 61 (2006) 999–1004.
- [17] <http://online.pheur.org/entry.htm>.
- [18] A. Othman, J.S.O. Evans, I.R. Evans, R.K. Harris, P. Hodgkinson, *J. Pharm. Sci.* 96 (2007) 1380–1397.